# High Coverages of Hydrogen on (10,0), (9,0) and (5,5) Carbon Nanotubes

**ARTICLE** *in* NANO LETTERS · FEBRUARY 2002

Impact Factor: 13.59 · DOI: 10.1021/nl020283o



**2 AUTHORS:**

C. W. Bauschlicher
NASA
**759** PUBLICATIONS **23,980** CITATIONS
SEE PROFILE

Christopher Richard So
United States Naval Research Laboratory
**22** PUBLICATIONS **454** CITATIONS
SEE PROFILE

NANO LETTERS

2002
Vol. 2, No. 4
337−341

# High Coverages of Hydrogen on (10,0), (9,0) and (5,5) Carbon Nanotubes

**Charles W. Bauschlicher, Jr.* and Christopher R. So†**

*NASA Ames Research Center, Moffett Field, California 94035*

*Received January 8, 2002; Revised Manuscript Received February 7, 2002*

**ABSTRACT**

**The binding energies of H to (9,0) and (5,5) carbon nanotubes are calculated for 50 and 100% coverages using the AM1 and/or ONIOM approaches. These results are compared to our previous results for hydrogen on the outside of a (10,0) tube. The average C–H binding energies for the optimal pattern are similar for all three tubes. For the (10,0) tube, 100% hydrogen coverage, with 50% on the inside and 50% on outside of the tube, is studied. The average C–H bond energy for this configuration is significantly larger than for hydrogen only on the outside at either 50% or 100% coverage.**

**I. Introduction.** We have recently studied the binding of hydrogen on the outside of a (10,0) carbon nanotube at low[1] and high[2] coverages using the ONIOM method.[3−5] This work was motivated, in part, by the recent interest in hydrogen storage in carbon nanotubes.[6−12] We found that 50% coverage on the outside of the tube appeared to be stable compared with the bare tube and $H_2$ molecules. It was found that patterns were much more stable than random coverages, and this was explained in terms of delocalized $\pi$ bonding and the need for $sp^3$ hybridization to form strong C−H bonds. At 100% coverage, the C−H binding was less favorable than the formation of $H_2$ molecules.

Very recently, Khare et al.[13] reacted nanotubes with atomic hydrogen and observed the C−H stretching mode. This experiment demonstrates that covalent C−H bonds are being formed. In light of this experimental study, we have extended our computational studies. In this manuscript we consider if these results are unique to the (10,0) tube or if other tubes with about the same diameter yield similar results. We also consider how the H patterns change with the type and size of the tube. For the (10,0) tube, we extend our previous work to include H bound on the inside and outside of the tube.

**II. Model and Methods.** The (5,5) and (9,0) tubes are approximately 10 Å long. Their ends are capped with half of a $C_{60}$ buckyball. This is different from our previous work[1,2] on a (10,0) tube, where the dangling bonds at the ends were tied off with hydrogen atoms. Using the caps makes the ends of the tubes stiffer and speeds up the geometry optimization procedure.

For 50% coverage on the (10,0) tube, we found[2] that patterns were significantly more stable than random coverages. This is consistent with the observation that F on the outside[14] and I on the inside[15] of carbon nanotubes have distinct, rather than random, patterns. Therefore, for the 50% coverage on the outside of the (9,0) and (5,5) tubes, we investigate several different patterns. For the 100% coverage of the (10,0) tube, with 50% on the inside and 50% on the outside, we consider extensions of the two most stable patterns found previously. The patterns are discussed in more detail below.

The AM1 and the two-level ONIOM approach[3−5] are used. The ONIOM approach is a mixed, two-level approach that treats a small section of the system accurately and the rest at a lower level. The present calculations combine the universal force field[16] (UFF), for the low-level treatment, with density functional theory (DFT) for the high-level description. For the DFT, we use the hybrid[17] B3LYP[18] functional in conjunction with the 6-31G basis set.[19] The AM1 calculations are performed using a modified version of Gaussian 94, where damping is used to obtain convergence. The ONIOM calculations are performed using Gaussian 98.[20]

In our previous study[1] we found that the AM1 binding energies were only qualitative in accuracy, with several of the structures being much more stable at the AM1 level than at the ONIOM level. At appears that the AM1 level does not treat localized and delocalized $\pi$ bonding equivalently. Thus the AM1 is used only to explore possible structure and the ONIOM approach is used to determine our best estimate for the binding energy. For hydrocarbons, B3LYP bond energies commonly have errors of less than 5 kcal/mol, and we expect the ONIOM bond energies to be of similar accuracy.

The geometries are fully optimized at the AM1 and ONIOM levels of theory. In the ONIOM calculations, twenty-four carbon atoms, at the center of the nanotube, are

* Corresponding author. E-mail: bauschli@pegasus.arc.nasa.gov. Space Technology Division, Mail Stop 230−3.
† ELORET Corp., Mail Stop 230-3.

10.1021/nl020283o CCC: $22.00 
**Published on Web 03/03/2002**

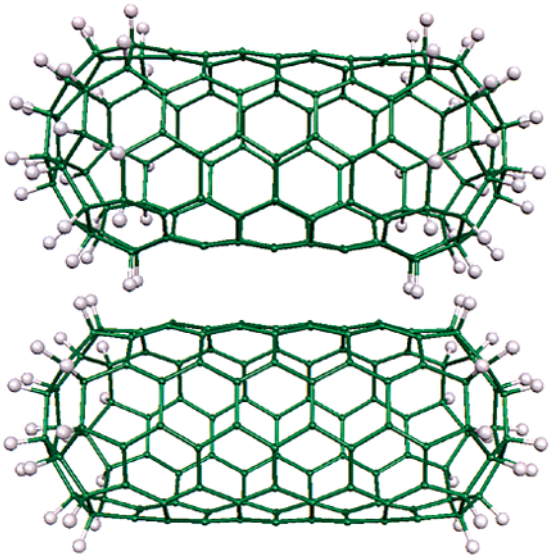

**Figure 1.** Comparison of the caps(40) and caps(60) models for the (5,5) tube.

used for the high-level treatment. The link hydrogen atoms and the chemisorbed hydrogen atoms are also in the high-level treatment. The atoms included in the high-level treatment are the same as used in our previous treatments.[1,2]

As noted in our previous study,[1] we encounted problems with local minima for the UFF description of the carbon nanotube, and therefore we use the B3LYP energies instead of the ONIOM energies, since the B3LYP energies were insensitive to the UFF solution. That is, we only use the molecular mechanics approach to constrain the shape of the high-level fragment.

**III. Results and Discussion.** The (5,5) and (9,0) tubes are both capped by $C_{30}$, which is half of a $C_{60}$ buckyball. The end of the (5,5) tube is a pentagon, while the end of the (9,0) tube is a hexagon. For the AM1 optimized (5,5) tube, there are clearly 20 atoms in each cap with approximately the same curvature as found in $C_{60}$, there are 10 carbon atoms that are bonded to the tube on one side and the cap on the other, and the remaining carbons are clearly in the tube. Since the 10 interface atoms could be considered as either in the tube or the cap, we partition the tube in two ways: (1) 40 capping atoms and 90 side-wall atoms and (2) 60 capping atoms and 70 side-wall atoms. The structures with H atoms attached only to these two cap definitions are denoted as "caps(40) only" and "caps(60) only", respectively, and are shown in Figure 1. For the (9,0) tube, there are 21 atoms clearly in the cap. The next ring of 18 carbons, which zigzags around the tube, would be assigned 9 to the cap and 9 to the side wall if the $C_{30}$ definition of the cap is used. However, the distance to the end of the tube is very similar for these carbon atoms, and therefore we assign all 18 to the cap, which leads to 39 carbon atoms being assigned to each cap, or a total of 78 cap atoms and 72 side-wall atoms.

The average tube-H bond energies are reported in Table 1. The AM1 average binding energies for the 100% coverage case for the (5,5) and (9,0) tubes are similar; see Table 1. The "caps only" values are larger than the 100% coverage result, while the "side-walls only" values are smaller. This is consistent with the higher curvature for the caps, which results in a smaller cost for the $sp^3$ hybridization and thus stronger C−H bonds for the caps. We also note that the caps(60) only value is smaller than the caps(40) only value, because the 20 boundary carbon atoms have some neighbors in the tube and some in the cap and therefore their curvature is smaller than for the true capping atoms. The (9,0) side-walls only value (44.0 kcal/mol) is similar to our previous value (46.8 kcal/mol) for the (10,0) tube, while the (5,5) side-wall(60) only value is slightly larger (47.1 kcal/mol).

**Table 1:** Summary of Average Binding Energies for Hydrogen on the outside of (10,0), (9,0), and (5,5) Nanotubes, in kcal/mol

| tube | AM1 | ONIOM |
|---|---|---|
| 100% (5,5) | 52.7 | |
| caps(40) only (5,5) | 67.4 | |
| side-wall(40) only (5,5) | 50.2 | |
| caps+side-wall (5,5) | 55.5 | |
| caps(60) only (5,5) | 64.9 | |
| side-wall(60) only (5,5) | 47.1 | |
| caps+side-walls(60) (5,5) | 55.3 | |
| 100% (5,5) longer tube | 52.1 | |
| caps only (5,5) longer tube | 67.8 | |
| side-wall only (5,5) longer tube | 49.7 | |
| caps+side-wall (5,5) longer tube | 54.9 | |
| 50% zigzag (5,5) | 59.1 | 58.4 |
| 50% pairs of lines (5,5) | 58.6 | 42.8 |
| 50% rings (5,5) | 51.8 | |
| 2H's perpendicular | | 37.2 |
| 2H's 30° | | 41.6 |
| 100% (9,0) | 51.3 | |
| caps only (9,0) | 58.5 | |
| side-wall only (9,0) | 44.0 | |
| caps+side-wall (9.0) | 51.5 | |
| 50% triple lines (9,0) | 64.2 | 62.4 |
| 50% single line (9,0) | 54.4 | 52.8 |
| 50% spiral (9,0) | 50.5 | 43.3 |
| 2H's parallel | | 44.5 |
| 2H's 60° | | 41.6 |
| side-wall only (10,0)[a] | 46.8 | 38.7 |
| 50% spiral (10,0)[a] | 58.3 | 52.6 |
| 50% pairs of lines (10,0)[a] | 58.3 | 57.3 |

[a] Taken from ref 2.

While the average side-wall C−H binding energy is similar for the three tubes, we observe that the weighted average of the caps and side-wall C−H binding energies for the (5,5) tubes, for both caps(40) and caps(60), are larger than average C−H bonds in the 100% coverage case. For the (9,0) tube, the difference is quite small. It should be noted that for the (5,5) tubes with 130 C−H bonds, the differences (2.8 and 2.6 kcal/mol) in the average bond energies corresponds to a total difference in binding energy of 369 or 337 kcal/mol. Since this difference is not strongly dependent on the cap definition, we test to see if it is related to the length of the tube. Our approximately 10 Å (5,5) tube has side-walls that are nine carbons long. In a test, we add an additional ring of carbons (see Figure 2), thus making the wall section of the tube 10 carbon atoms long, yielding a $C_{140}$ tube. As can be seen in Table 1, increasing the length of the tube has only a very small effect on the results. Thus the difference between

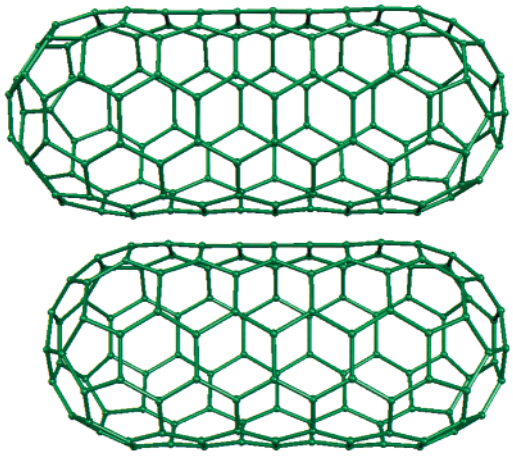

**Figure 2.** Comparison of the two different length (5,5) tubes studied in this work.

the 100% value and the weighted average of the caps and side walls does not appear to be affected by the length of the tube. We therefore conclude that there is an interaction between the caps and side-wall hydrogens that reduce the average C−H binding energy for the 100% coverage of the (5,5) tube.

An inspection of the tubes shows that the C−C bond length increases from about 1.4 to about 1.5 Å when the C−H bonds are present. Thus adding the side-wall hydrogens increases the diameter of the tube, while adding only the cap hydrogens lengthens the tubes slightly and gives them a slight dumbbell shape. This is true for both the (5,5) and (9,0) tubes, but the distortion appears a bit larger for the (9,0) tube. Despite the apparently larger distortion for the (9,0) tube, it is the (5,5) tube that shows some repulsive interaction between the cap hydrogens and the side-wall hydrogens. To study the chemistry of the side walls, we clearly need to remove the effect of the caps which have a larger binding energy than the side walls and can indirectly affect the side-wall H's at the cap−tube interface. In our ONIOM treatment, the high-level section contains only side-wall atoms, but the end of the high-level section can be adjacent to the atoms that can be assigned to the caps. Thus our tubes must be considered as essentially the minimum size needed to study these systems.

As discussed previously, $sp^3$ hybridization is required to form strong C−H bonds, which results in the carbons bonded to the H atoms bulging out of the tube. A hydrogen coverage of 100% is not favorable relative to the formation of $H_2$, because it is not possible for every carbon to achieve a tetrahedral-like geometry. Lee and Lee[11] found 100% C−H coverage inside the tube to be less favorable than the formation of $H_2$. We suggested[2] that maximum hydrogen coverage of 50%, where half of the carbons bulge out of the tube and form a strong C−H bond, while the remaining carbons move inward and retain the $\pi$ bonding. Since it is favorable to retain the delocalized $\pi$ bonding with good p$\pi$−p$\pi$ overlaps, we found patterns for a (10,0) tube where the hydrogen atoms were located along the axis of the tube or spiraled around the tube were the most favorable. In this work we also consider patterns for the (5,5) and (9,0) tubes.

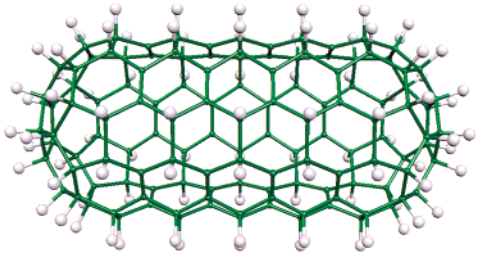

**Figure 3.** Our model for the pairs of lines pattern of 50% hydrogen coverage on the (5,5) tube.

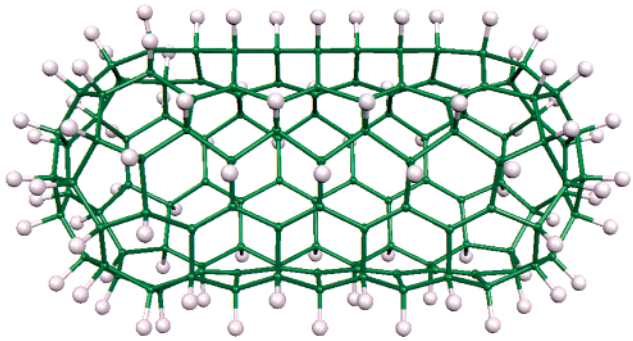

**Figure 4.** Our model for the zigzag pattern of 50% hydrogen coverage on the (5,5) tube.

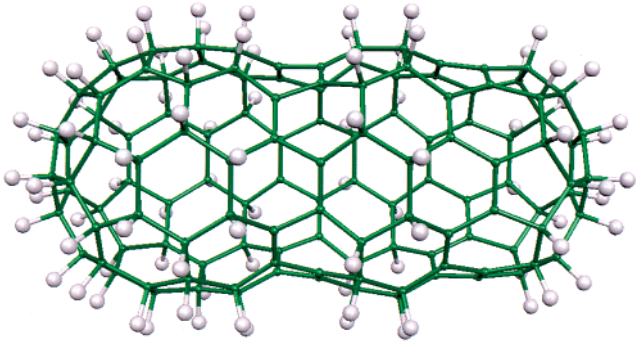

**Figure 5.** Our model for the rings pattern of 50% hydrogen coverage on the (5,5) tube.

For the (5,5) tube, we consider three patterns, "pairs of lines", "zigzag", and "rings", which are shown in Figures 3−5. We should note that for the (5,5) tube, we are unable to construct a spiral pattern due to the number of atoms in the circumference of the tube. The AM1 binding energies for pairs of lines and zigzag patterns are similar and the rings pattern is much less favorable. This is consistent with the results for the (10,0) tube, where ring structures are less favorable than those with the H atoms running along the axis of tube since the p$\pi$−p$\pi$ overlap is smaller for rings than when the $\pi$ bonds are along the tube; thus the bonding in the bare tube sections is weaker for the ring structures. We expect this to be true for all types of tubes and therefore do not consider the ring structures further.

When the ONIOM approach is used to compute the binding energy, the zigzag structure is much more favorable than the pairs of lines. This arises because the zigzag structure

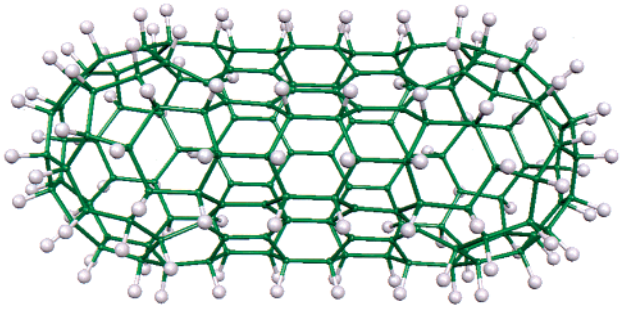

**Figure 6.** Our model for the triple lines pattern of 50% hydrogen coverage on the (9,0) tube.

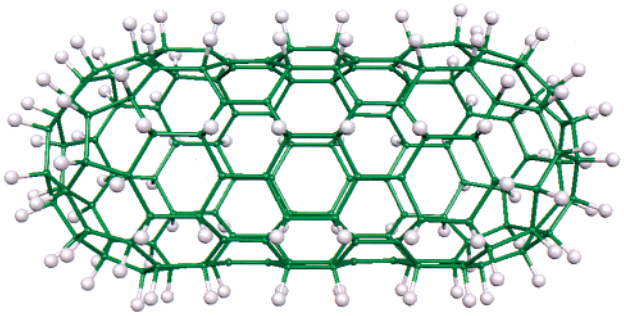

**Figure 7.** Our model for the single line pattern of 50% hydrogen coverage on the (9,0) tube.

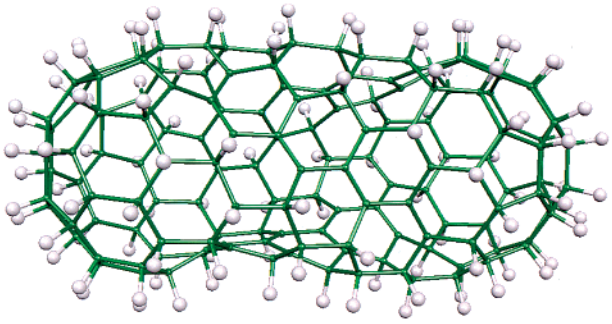

**Figure 8.** Our model for the spiral pattern of 50% hydrogen coverage on the (9,0) tube.

has delocalized $\pi$ bonds while the pairs of lines has localized $\pi$ bonds, and the higher level ONIOM approach favors the structure with delocalized $\pi$ bonds. We also observed this effect for the (10,0) tube. This change in relative stability with level of theory illustrates why one must go beyond the AM1 approach.

For the (9,0) tube we consider three patterns, "triple lines", "single lines", and "spiral", which are shown in Figures 6−8. Because the number of carbon atoms in a ring around the tube is not divisible by 4, it is not possible to make pairs of lines as found for the (10,0) tube. However, the number of carbons is divisible by two and six and we can create structures with a repeating unit of one line of H and one line of $\pi$ bonds, denoted as single lines, and a repeating unit of three lines of hydrogens and three lines of $\pi$ bonds, denoted as triple lines. The change in the number of carbon atoms in the ring circumference also means that it is not possible to create a pattern with a repeating unit of one spiral of hydrogens and one spiral of pi bonds. The spiral pattern

**Table 2:** Summary of the Average Hydrogen Binding Energies for the (10,0) Tube, in kcal/mol, Computed Using the ONIOM Approach

| tube | all H's | inside H's only |
|---|---|---|
| 100% outside | 38.7 | |
| 50% outside spiral | 52.6 | |
| 50% outside pairs of lines | 57.3 | |
| 100% spiral (50% inside) | 74.6 | 96.5 |
| 100% pairs of lines (50% inside) | 77.4 | 97.5 |

we consider has a repeating unit of one and half spirals of hydrogen and one and half spirals of $\pi$ bonds. At both AM1 and ONIOM levels the triple lines is the most favorable and the spiral the least favorable. In the triple lines, three lines of carbons bulge out of the tube to improve their hybridization and hence form strong C−H bonds. The three bare rows of carbon atoms flex in and form a planar region with delocalized $\pi$ bonding. This is very similar to the very favorable pairs of lines for the (10,0) tube.

At the ONIOM level, the binding energies for the most favorable patterns for the three tubes studied are 58.4 (5,5), 62.4 (9,0), and 57.3 kcal/mol (10,0). The (5,5) and (9,0) tubes have approximately the same curvature, and this suggests that zigzag tubes have larger binding energies than arm chair tubes for the same diameter tube; however, additional tubes need to be studied to confirm this. The (9,0) C−H binding energy is larger than the (10,0) binding energy, which is consistent with the larger curvature for the (9,0) tube. However, it must be remembered that the patterns are different for these two tubes because the change in the number of carbons around the tube.

In addition to the 50% coverage cases, we consider only two hydrogen atoms bound to the (5,5) and (9,0) tubes. The hydrogens are on adjacent carbon atoms, yielding two possible structures for each tube; these are identified by the orientation of a line connecting the two hydrogens with respect to the tube axis. For the (5,5) tube, it is better to orient the H atoms with a 30° angle rather than with a 90° angle with respect to the tube axis. For the (9,0) tube, the orientation with the H atoms parallel to the tube axis is favored over the 60° orientation. Thus, even for the low coverage, the most favorable orientation of the hydrogens is along the tube.

The binding energies for the three tubes studied are sufficiently similar that we conclude that H bonding to the side wall of the tube is not strongly dependent on the type of the tube for similar diameter tubes, but the most favorable pattern will depend on the type of the tube. The most favorable structure has the hydrogens running along the tube rather than around the tube, and have delocalized $\pi$ bonding that also runs along the length of the tube.

In our previous study[2] of the (10,0) tube, we found that the two most stable patterns were the pair of lines and spiral. In this work, we study these two structures at 100% coverage, where 50% of the hydrogens are on the outside and 50% are on the inside of the tube. That is, the hydrogens are bonded to the inside of the tube on what was previously the bare carbon atoms. The binding energies are summarized in

Table 2. The binding energies of the inside H atoms for both patterns are much larger than found for the H atoms on the outside. That is, the H atoms on the outside, distort the tube such that the bare carbons have their p orbitals pointing inward with significant $sp^3$ character; thus their C−H binding energies are close to the typical 100 kcal/mol for aliphatic carbon. This is in distinct contrast to 100% on the outside where the average bond energies decreases significantly between 50% and 100% coverage. Thus 100% hydrogen coverage is favorable if 50% is on the inside of the tube. This result does not address the question of how to get hydrogen inside the tube, but we note that Ma et al.[12] have suggested that bombarding tubes with H atoms could deposit H on the inside of the tube.

We have explored the stability of some isolated nanotubes with high coverages of hydrogen. While we have found that high coverages of hydrogen are possible, this is only the first step in determining their suitability for hydrogen storage. For a practical storage system, it must be possible to add and remove the hydrogen. To investigate this in detail would require the determination of the barrier for the loss of two H atoms leading to the production of $H_2$. While we have not performed this computationally intensive calculation; some exploratory calculations suggest a barrier in the range of 40−70 kcal/mol for addition or loss of $H_2$. Thus a catalysis might be required to facilitate the addition and removal of $H_2$. In addition, the interaction of the tube with a realistic environment might affect the stability of the tube and any barriers for the loss of addition of $H_2$, and this is not addressed in our calculations. However, the experiments of Khare et al.[13] suggest that the interaction does not lead to a low-energy path for the loss of $H_2$.

**IV. Conclusions.** For 50% coverage, we find that the most favorable patterns have similar binding energies for the (5,5), (9,0), and (10,0) tubes. The (9,0) result is slightly larger than the (10,0) value, probably due to the greater curvature for the smaller tube. The (5,5) value is smaller than the (9,0) value, suggesting that for the same size tube, the zigzag tubes have a larger binding energy than arm chair tubes. We find that while 100% coverage on the outside of the tube is unfavorable, 50% on the inside and 50% on the outside of the tube is a very favorable bonding situation. The 100% coverage represents a hydrogen storage of about 8 wt %.

**Acknowledgment.** We acknowledge the help of Whalen Rozelle in generating the nanotube coordinates.

## References

(1) Bauschlicher, C. W. *Chem. Phys. Lett.* **2000**, *322*, 237.
(2) Bauschlicher, C. W. *Nano. Lett.* **2001**, *1*, 223.
(3) Svensson, M.; Humbel, S.; Froese, R. D. J.; Matsubara, T.; Sieber, S.; Morokuma, K. *J. Phys. Chem.* **1996**, *100*, 19357.
(4) Humbel, S.; Sieber, S.; Morokuma, K. *J. Chem. Phys.* **1996**, *105*, 1959.
(5) Maseras, F.; Morokuma, K. *J. Comput. Chem.* **1995**, *16*, 1170.
(6) Chen, P.; Wu, X.; Lin, J.; Tan, K. L. *Science* **1999**, *285*, 91.
(7) Ye, Y.; Ahn, C. C.; Witham, C.; Fultz, B.; Liu, J.; Rinzler, A. G.; Colbert, D.; Smith, K. A.; Smalley, R. E. *Appl. Phys. Lett.* **1999**, *74*, 2307.
(8) Simonyan, V. V.; Diep, P.; Johnson, J. K. *J. Chem. Phys.* **1999**, *111*, 9778.
(9) Dillon, A. C.; Jones, K. M.; Bekkedahl, T. A.; Kaing, C. H.; Behmune, D. S.; Heben, M. J. *Nature* **1997**, *386*, 377.
(10) Froudakis, G. E. *Nano Lett.* **2001**, *1*, 179.
(11) Lee. S. M.; Lee, Y. H. *Appl. Phys. Lett.* **2000**, *76*, 2000.
(12) Ma, Y.; Xia, Y.; Zhao, M.; Wang, R.; Liangmo, M. *Phys. Rev. B.* **2001**, *63*, 115422.
(13) Khare, B. N.; Meyyappan, M.; Cassell, A. M.; Nguyen, C. V.; Han, J. *Nano Lett.* **2002**, *2*, 73.
(14) Kelly, K. F.; Chiang, I. W.; Mickelson, E. T.; Hauge, R. H.; Margrave, J. L.; Wang, X.; Scuseria, G. E.; Radloff, C.; Halas, N. J. *Chem. Phys. Lett.* **1999**, *313*, 445.
(15) Fan, X.; Dickey, E. C.; Eklund, P. C.; Williams, K. A.; Grigorian, L.; Buczko, R.; Pantelides, S. T.; Pennycook, S. J. *Phys. Rev. Lett.* **2000**, *84*, 4621.
(16) Rappe, A. K.; Casewit, C. J.; Colwell, K. S.; Goddard, W. A.; Skiff, W. M. *J. Am. Chem. Soc.* **1992**, *114*, 10024.
(17) Becke, A. D. *J. Chem. Phys.* **1993**, *98*, 5648.
(18) Stephens, P. J.; Devlin, F. J.; Chabalowski, C. F.; Frisch, M. J. *J. Phys. Chem.* **1994**, *98*, 11623.
(19) Frisch, M. J.; Pople, J. A.; Binkley, J. S., *J. Chem. Phys.* **1984**, *80*, 3265 and references therein.
(20) Frisch, M. J.; Trucks, G. W.; Schlegel, H. B.; Scuseria, G. E.; Robb, M. A.; Cheeseman, J. R.; Zakrzewski, V. G.; Montgomery, J. A., Jr.; Stratmann, R. E.; Burant, J. C.; Dapprich, S.; Millam, J. M.; Daniels, A. D.; Kudin, K. N.; Strain, M. C.; Farkas, O.; Tomasi, J.; Barone, V.; Cossi, M.; Cammi, R.; Mennucci, B.; Pomelli, C.; Adamo, C.; Clifford, S.; Ochterski, J.; Petersson, G. A.; Ayala, P. Y.; Cui, Q.; Morokuma, K.; Malick, D. K.; Rabuck, A. D.; Raghavachari, K.; Foresman, J. B.; Cioslowski, J.; Ortiz, J. V.; Stefanov, B. B.; Liu, G.; Liashenko, A.; Piskorz, P.; Komaromi, I.; Gomperts, R.; Martin, R. L.; Fox, D. J.; Keith, T.; Al-Laham, M. A.; Peng, C. Y.; Nanayakkara, A.; Gonzalez, C.; Challacombe, M.; Gill, P. M. W.; Johnson, B. G.; Chen, W.; Wong, M. W.; Andres, J. L.; Head-Gordon, M.; Replogle, E. S.; Pople, J. A. *Gaussian 98*, revision A.7; Gaussian, Inc.: Pittsburgh, PA, 1998.

NL020283O